2014

Spin polarization asymmetry at the surface of chromia

Shi Cao
University of Nebraska-Lincoln, caoshi86@gmail.com

Xin Zhang
University of Nebraska-Lincoln, s-xzhang19@unl.edu

Ning Wu
University of Nebraska-Lincoln

A T. N'Diaye
Lawrence Berkeley National Laboratory

G Chen
Lawrence Berkeley National Laboratory

See next page for additional authors

Spin polarization asymmetry at the surface of chromia

2014 New J. Phys. 16 073021

(http://iopscience.iop.org/1367-2630/16/7/073021)

New Journal of Physics
The open access journal at the forefront of physics
Deutsche Physikalische Gesellschaft DPG | IOP Institute of Physics

Spin polarization asymmetry at the surface of chromia

Shi Cao[1], Xin Zhang[1], Ning Wu[1], A T N'Diaye[2], G Chen[2], A K Schmid[2], Xumin Chen[1], W Echtenkamp[1], A Enders[1], Ch Binek[1] and P A Dowben[1]

[1] Department of Physics and Astronomy, Nebraska Center for Materials and Nanoscience, University of Nebraska, Lincoln, Nebraska 68588, USA
[2] NCEM, Lawrence Berkeley National Laboratory, Berkeley, California 94720, USA
E-mail: pdowben@unl.edu

Received 28 March 2014, revised 10 June 2014
Accepted for publication 12 June 2014
Published 17 July 2014

New Journal of Physics **16** (2014) 073021

doi:10.1088/1367-2630/16/7/073021

Abstract

We demonstrate boundary spin polarization at the surface of a Cr_2O_3 single crystal using spin-polarized low-energy electron microscopy (SPLEEM), complementing prior spin polarized photoemission, spin polarized inverse photoemission, and x-ray magnetic circular dichroism photoemission electron microscopy measurements. This work shows that placing a Cr_2O_3 single crystal into a single domain state will result in net Cr_2O_3 spin polarization at the boundary, even in the presence of a gold overlayer. There are indications that the SPLEEM contrast for the two polarization states may be different, consistent with scanning tunneling microscopy spectroscopy results obtained from ultrathin films of Cr_2O_3.

Keywords: magnetoelectrics, surface spin polarization, voltage control of spin, surface and interface dipoles

Introduction

The predicted boundary spin polarization [1–3] at the surface of magnetoelectric chromia, $Cr_2O_3(0001)$, was confirmed experimentally by the combination of spin polarized photoemission [3], spin polarized inverse photoemission [4], x-ray magnetic circular dichroism photoemission electron microscopy [4] and magnetic force microscopy [4]. The presence of roughness insensitive boundary magnetization in chromia's antiferromagnetic single domain

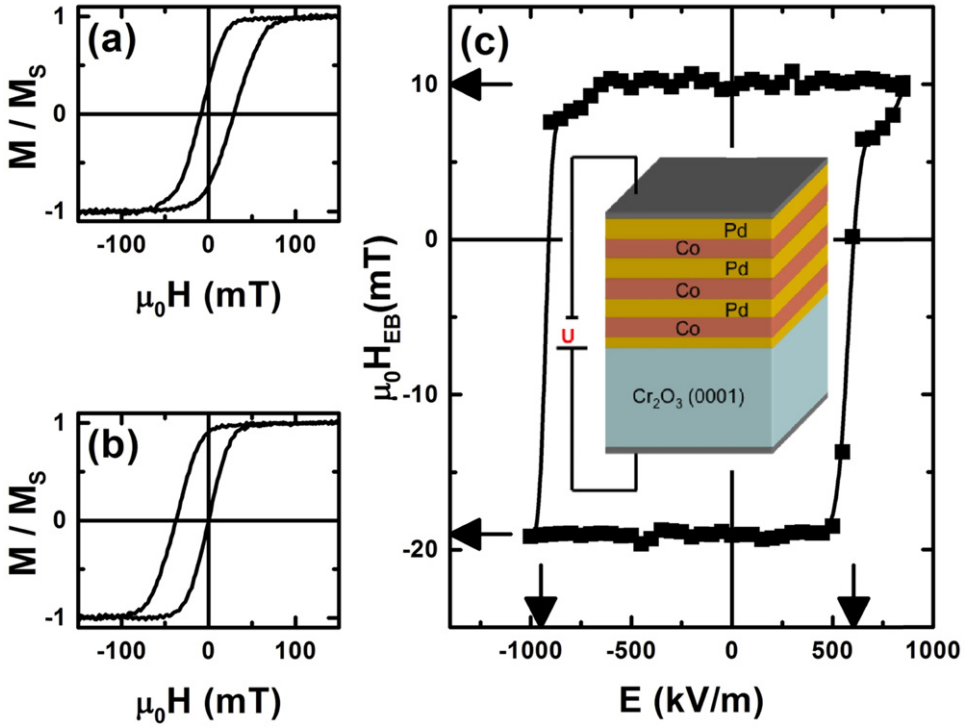

Figure 1. Hysteresis loop of pinned CoPd multilayer thin film on chromia (Cr_2O_3), as schematically shown in the insert, measured at $T = 303$ K (a) in the positive exchange bias saturation state and (b) the negative exchange bias saturation state. (c) Hysteretic behavior of equilibrium exchange bias measured after the system has been initialized by applying an electric field, E, and a constant magnetic field of 400 mT. Asymmetry relative to $H_{EB} = 0$ and $E = 0$ are indicated by horizontal and vertical arrows.

state in concert with the fact that the boundary magnetization can be switched by electrical means makes the magnetoelectric antiferromagnet chromia a prototypical candidate for electrically controlled exchange bias [5]. Yet the exchange bias field, H_{EB}, in a bilayer of chromia and an adjacent exchange coupled ferromagnetic thin film (as seen in figure 1), observed after isothermal switching through an applied electric field, E, in the simultaneous presence of a constant magnetic field, was found to differ in magnitude between the $Cr_2O_3(0001)$ single domain states of opposite surface/interface magnetization [3, 6]. In addition to asymmetry in the magnitude of the exchange bias field on switching there is an asymmetry in the magnitude of the electric switching fields required to switch from positive to negative exchange bias and vice versa [7]. The latter asymmetry is consistent with early findings of Martin and Anderson [8]. Martin and Anderson [8] introduced the concept of seed domains to explain Barkhausen-type jumps in the magnetoelectric susceptibility hysteresis near the electric coercive field in the isothermal switching of the magnetoelectric susceptibility. The susceptibility hysteresis accompanies the isothermal switching between the two antiferromagnetic domain states of a chromia single crystal. While it seems straightforward to assume that in the case of chromia based exchange bias, seed domains in the chromia pinning layer favor one domain state over the other in the isothermal switching of the domain state [7, 8], the experimental picture is, in fact, less clear. Extensive investigations and comparison between complete and partial isothermal switching in chromia based voltage-controlled exchange bias

heterostructures show that the magnitude of the exchange bias field near its maximum values is not a rigorous measure to determine whether the antiferromagnet is in a true single domain state or if unreversed seed domains are present [6]. Careful consideration [7] of the asymmetry in the magnitude of the exchange bias field in concert with the asymmetry between the switching fields requires an assumption about local variations in the interface exchange. Specifically, a consistent explanation of the simultaneous presence of both asymmetry in the switching field and in the magnitude of the exchange bias, as summarized in figure 1(c), requires that the exchange interaction between the interface magnetization of the seed domains is antiferromagnetic while the rest of the boundary magnetization couples ferromagnetically with the ferromagnet. Indeed positive exchange bias originating from antiferromagnetic interface coupling has been observed in chromia based exchange bias heterostructures making such a scenario likely [9]. There has been no direct evidence, however, that the seed domains proposed by Martin and Anderson have an effect on surface properties and create an asymmetry in the boundary magnetization between the two electrically switched antiferromagnetic domain states of a chromia (0001) thin film.

Once chromia is in a heterojunction structure with a ferromagnetic metal, or any conductor, a permanent interface dipole results from the breaking of translation symmetry of the electronic potential. The electric field associated with this dipole does not switch on reversal of the antiferromagnetic domain state. It therefore breaks the symmetry by favoring one domain state over the other when it superimposes with the applied positive or negative electric field to form the local field which determines via magnetoelectric response the magnitude of the boundary magnetization. Certainly results [3, 6] obtained for chromia in contact with a ferromagnetic metal do not exclude the interface static electric dipole as a contributing factor to the asymmetry in the switching field and/or in the magnitude of the exchange bias of one domain state over the other, so the interface must therefore be considered as a possible contributor to the asymmetry. The interface is likely important as a solely bulk measurement may exhibit no asymmetry in the switched magnetization [10].

It is the objective of this investigation to provide evidence for the asymmetry in the boundary magnetization through surface sensitive spectroscopy and shed some light on the origin of this symmetry breaking. To better characterize the net Cr_2O_3 spin polarization at the boundary, we want to observe differences in the absolute magnitude for the spin polarization for the two domain states for a chromia single crystal under a thin conducting overlayer and for a chromia thin film on top of a conducting substrate. We find indications of these contrast variations in spin-polarized low-energy electron microscopy (SPLEEM) and this finding is consistent with our results from scanning tunneling microscopy and spectroscopy (STM, STS).

Methods and experimental details

Cr_2O_3(0001) single crystal surfaces were prepared under ultrahigh vacuum conditions by Ar ion sputtering at 2 keV for a half hour followed by annealing, similar to prior work [3, 4]. To place the Cr_2O_3(0001) single crystal in a single domain state [3–6], the sample was field cooled through the Néel temperature of 308 K in the presence of both an electric field ($\sim$5 kV mm^{-1}) and magnetic field ($\sim$50 Gauss). The magnetic field was applied either parallel or anti-parallel to the applied electric field.

SPLEEM [11, 12] was used to measure the spin-dependent electron reflectivity of the $Cr_2O_3(0001)$ surface. The spin-dependent reflectivity difference is expressed as an asymmetry signal $A = (I_+ - I_-)/(I_+ + I_-)$, where $I_\pm$ stands for the reflectivity for the different spin orientations [11, 12]. The pixel-by-pixel asymmetry signal is computed from pairs of full-field reflectivity images obtained using opposite spin directions of the electron beam. To supply an interface to a conductor, four atomic monolayers of gold were deposited from an e-beam heated crucible evaporator onto the surface of the $Cr_2O_3(0001)$ single crystal at the rate of about 7 min per monolayer. Adding this chromia/metal interface has the added benefit of suppressing surface charging.

The experiments on the chromia thin films grown on Cu(111) were also performed in ultra-high vacuum. The Cu(111) single crystal of purity >99.999% was prepared by repeated cycles of Ar ion sputtering and annealing at a temperature of 850 K. The chromia thin film on the Cu (111) substrate was prepared by evaporation of two monolayers of metallic chromium onto the clean Cu(111) surface from an e-beam heated crucible evaporator, followed by annealing to 920 K for 1 min in a partial oxygen pressure at 5×10^{-7} Torr. As described elsewhere [13, 14], this leads to a very flat chromia thin film with pronounced texture along (0001) and little or no mosaic spread. Samples were imaged with a low-temperature scanning tunneling microscope (Omicron Nanotechnology). Topography images and spectroscopy maps were obtained under constant current mode at 77 K. Electrochemically etched polycrystalline W tips were cleaned in vacuo by annealing them at temperatures $T > 2200$ K. The tunneling spectroscopy maps were obtained by adding a modulation voltage $V_{mod} = 20$ mV rms to the applied bias voltage and recording the dI/dV signal by lock-in techniques. STM images were obtained at high bias voltages, typically −5.5 V, to overcome the significant 2.7 to 3.2 eV band gap of the films [15] and low density of states at the valence band maximum and especially the conduction band minimum [15, 16] to tunnel out of the conduction band of the chromia films.

Polarization asymmetry

The SPLEEM measurements were performed after cooling the chromia crystal through the Néel temperature. The SPLEEM asymmetry signal was found to be particularly pronounced at electron kinetic energies of about 10.2 eV, where relatively high electron reflectivity coincides with a strong (negative) asymmetry signal. Figure 2(a) shows a time-averaged SPLEEM image of the $Cr_2O_3(0001)$ surface (pixel-by-pixel average of 60 individual images), after the application of a ∼50 Gauss magnetic switching field applied on cooling from above the Néel temperature to below T_N. The uniform and featureless bright image indicates that the chromia surface is in a single domain state with spin-up boundary polarization. Figure 2(b) shows the same area of the surface prior to application of the switching field (again 60 frames were averaged): uniform dark field of the image indicates a boundary polarization switched into a spin-down single domain state. As evident from the uniform images and uniform contrast indicated by figures 2(a), (b), any unreversed seed domains at the chromia surface, i.e. the chromia gold overlayer interface, present must be smaller than roughly 100 nm.

The average asymmetry signal of individual SPLEEM images is plotted as a function of time in figure 2(c), where the black/solid and red/dashed lines show the asymmetry signal prior to and after the application of the switching field. These measurements show that the magneto-electric reversal of the chromia domain state is accompanied with a reversal of the surface

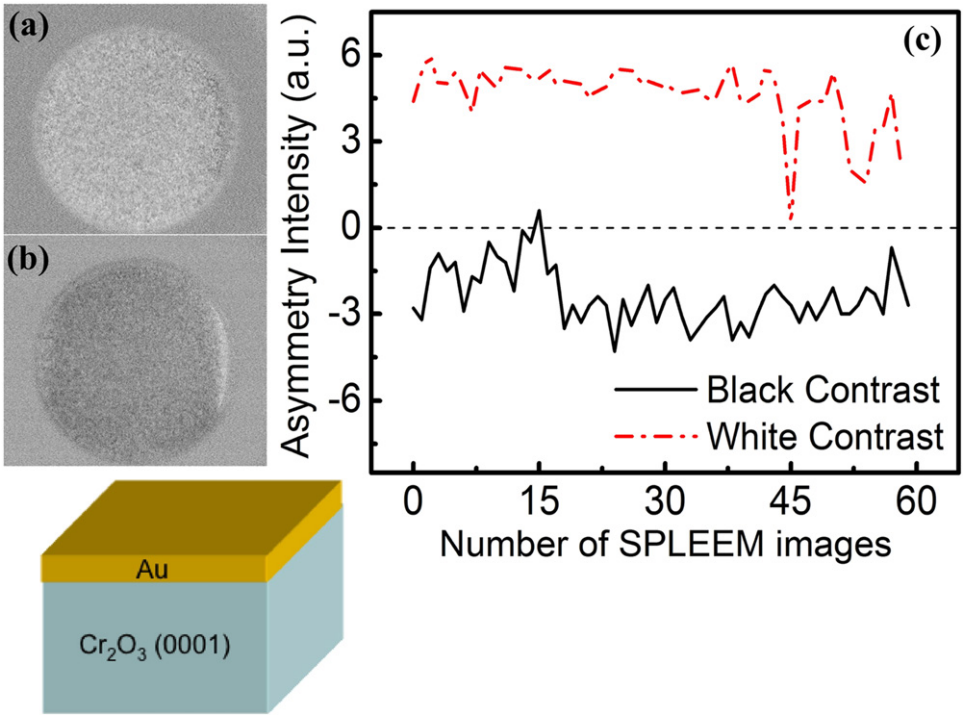

Figure 2. SPLEEM images of an area on the Cr_2O_3 surface, covered with a thin gold layer as shown in the schematic. The field of view is ~14 μm and the electron energy is 10.2 eV. Panels (a) and (b) show long-time exposures (pixel-by-pixel averages of 60 frames), after application of a switching magnetic field (~50 Gauss) and prior to application of the switching field. Brightness and darkness in the images indicate magnetic single domain states with spin up and down boundary polarization, respectively. (c) Time traces of the asymmetry signal: the black solid line corresponds to negative asymmetry before application of the switching field, and the dashed red line corresponds to positive asymmetry after the field pulse, indicating the switch of the spin orientation at the Cr_2O_3 surface.

polarization. The switching process also occurs isothermally below the Néel temperature, consistent with previous studies [3, 6].

The most striking observation is that the magnitude of asymmetry intensities is different for the opposite domain states and hence opposite surface polarizations (figure 2(c)). As noted at the outset, previous studies [3, 6] have indicated that the surface boundary magnetization states will produce a different magnitude of the exchange bias field in the $(Co/Pd)_n/Cr_2O_3$ system. A spin-up surface boundary domain state results in a two-fold larger exchange bias than a spin-down boundary domain state. The domain state dependence of the exchange bias coincides with the SPLEEM spin polarization asymmetry measurements which are roughly twofold larger in the spin up domain state than the spin down domain state polarization of the Cr_2O_3(0001) surface, as seen in figure 2(c).

If the variation in the magnitude of the spin polarization depends on the electrostatic interface dipole formed at the Cr_2O_3/metal boundary, then thickness variations in chromia films grown on a conducting metal substrate should matter as well. In the thin film limit, there should be thickness dependent variations in the magnitude of the surface magnetization on the vacuum

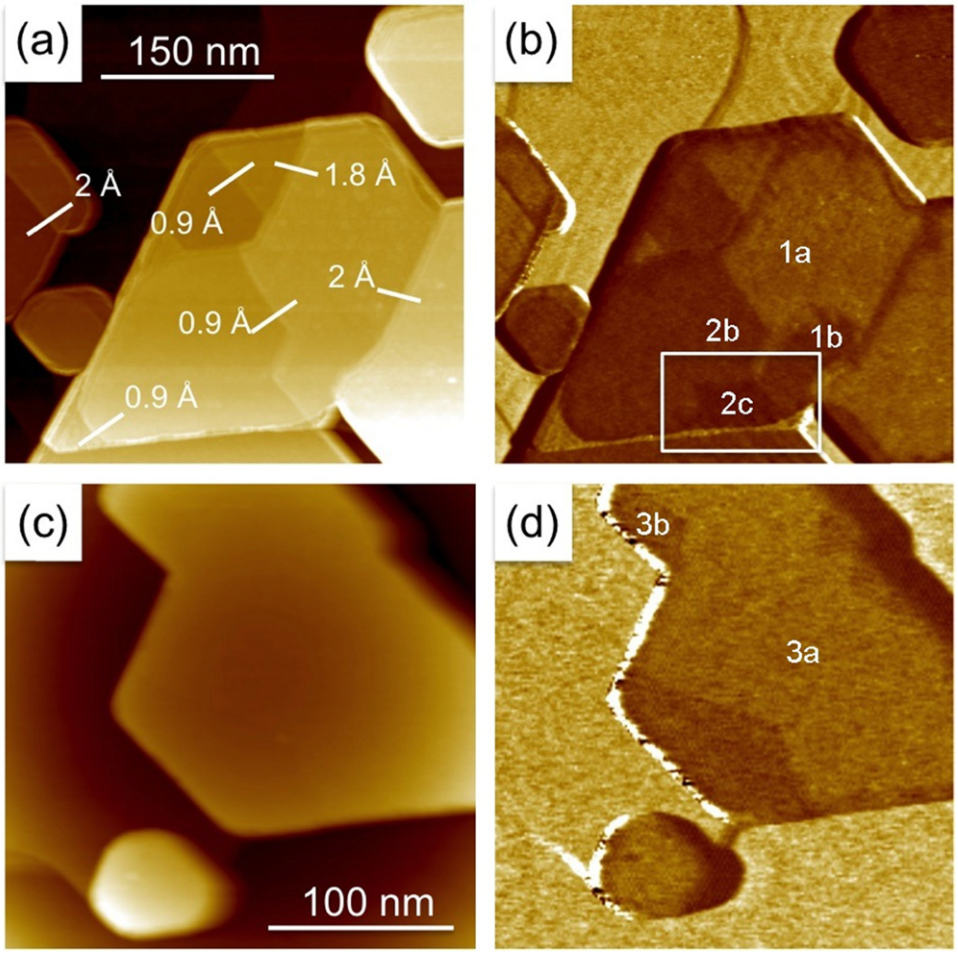

Figure 3. Scanning tunneling microscopy images (a), (c) and corresponding dI/dV tunneling spectroscopy maps (b), (d), of selected chromia islands on Cu(111). The oxidized Cu surface appears to have the highest local conductivity and appears brightest in the spectroscopy maps. There appears to be a strong correlation between the morphology of the chromia islands and the local conductivity in (a), (b), but not in (c), (d). Likewise, the contrast highlighted by a rectangle in (b) does not have a corresponding morphological feature in the island in (a); that is to say that (b)'s regions of contrast 1(a) and 1(b) or 2(b) and 2(c) have unequivocally no corresponding morphological features in (a) and the different contrasting areas 3(a) and 3 in (d) have unequivocally no corresponding morphological features in (c). In (b), 1(b) and 2(b) share the same conductivity but are separated in (a) by what appears to be a small step. Tunnel parameters: $U_B = -5.5$ V, $I_T = 0.2$ nA.

interface of a $Cr_2O_3(0001)$ thin film deposited on a conducting substrate, as screening of the electric interface dipole by the dielectric chromia is limited.

Variations in surface magnetization with chromia film thickness

STM images of very thin chromium oxide $Cr_2O_3(0001)$ films on Cu(111) are shown in figure 3. The island sizes are quite large [13], typically several micrometers, and the islands usually

extend over several substrate terraces. The Cu substrate is also visible between the islands. Also shown in figures 3(b), (d) are dI/dV spectroscopy maps, which were recorded simultaneously with the STM images. The conductivity of the oxidized Cu substrate is higher than the conductivity of the Cr_2O_3 islands so that they appear brightest in the spectroscopy maps. Importantly, the spectroscopy maps reveal contrast across the Cr_2O_3(0001) islands on Cu(111), which corresponds to domains of different local conductivity within those islands. These domains can in some instances be correlated with the morphology of the islands, as in figures 3(a), (b), and in other cases these domains exist without corresponding features in the island morphology, as in figures 3(c), (d) and in the highlighted area in figure 3(b). The terrace step heights in a selected island of Cr_2O_3 are indicated in figure 3(a), where it appears that two types of step heights exist, which are $2\,\text{Å} \pm 0.1\,\text{Å}$, and $0.9\,\text{Å} \pm 0.1\,\text{Å}$. Careful comparison with the local conductivity map in figure 3(b) suggests that terraces of different local conductivity are separated by the smaller steps, while terraces of similar local conductivity are separated by larger steps.

The observation of two types of step heights and local conductivities suggests that two characteristic surface terminations corresponding to different cuts through the Cr_2O_3 unit cell coexist. For instance, for the typical termination of Cr_2O_3, layer distances of Cr–O and O–Cr are about 0.94 Å. A complete layer of chromium atoms is actually rumpled a bit, so might be regarded as two layers, with the Cr–Cr layer spacing about 0.3 Å [17]. Two chemically equivalent (0001) surface terminations should occur in multiples of ~2.3 Å, which is the dimensions of the first four surface layers as Cr–O–Cr–Cr. The Cr–O layer spacing and the Cr–O–Cr–Cr layer spacing both seem to correspond reasonably well with the coexistence with both types of surface terminations. It should be noted, however, that the termination of the surface of Cr_2O_3 is much debated. Recent first principles calculations [18] suggest that the surface of Cr_2O_3 is Cr-terminated and thermodynamically stable in a broad temperature range between 165 K and well above room temperature, although detailed models invoking fractional Cr-layer occupancy have also been discussed [17, 19]. The predicted stability of Cr termination [18] clearly speaks against the coexistence of Cr- and O-terminated surfaces, consistent with experimental results [13, 20, 21]. Moreover, our frequent experimental observation of conductivity domains that do not correlate with steps in the film, such as those in figures 3(c), (d), as well as the highlighted region in figure 3(b), are also inconsistent with the assumption of variations in the surface termination.

As an alternative explanation, we suggest that there is a link between the two observed domains of local conductivity and the electrostatic surface dipole in the chromia film. This surface dipole effectively modulates the tunneling current and can explain the two types of conductivity domains observed here. Such a link between the orientation of electric polarization in a tunnel junction and the tunneling conductivity has been established in theory and experiment, and this is the fundamental contrast mechanism in the conductivity maps of the Cr_2O_3 islands here [22–24]. Importantly here, the total dipole moment of the Cr_2O_3 islands is directly coupled to its surface magnetization, so that the dI/dV maps shown in figures 3(b), (d) include information about both the intrinsic dipole and the surface spin polarization. The Cr_2O_3 islands show typically two to three different conductivities, which we believe correspond to the dipole of the film (up or down), modulated by the dipole associated with the interface magnetization (up or down). We note that STM measurements cannot be used to easily separate the dipole contributions at the surface and the buried copper-chromia interface, yet three out of the four possible expected contrast values expected are visible in figure 3(b).

An interpretation that needs to be explored further is the possibility of partial/incomplete antiferromagnetic domain reversal, as has been suggested [8] based on observations of multiple energy thresholds for domain reversal. While the antiferromagnetic domain reversal can occur uniformly under applied electric $\boldsymbol{E}$ and magnetic $\boldsymbol{B}$ fields, an interface dipole might lead to a diminished boundary polarization as a result of magneto-electric polarization of opposite sign from the static interface dipole, so that there is a type of frustrated ferroelectric domain reversal as a result of the interface dipole. This effect may be especially pronounced in the thin film limit. Partial domain reversal was suggested in [8], however, the influence of boundary polarization and interface dipoles was not considered. Interestingly enough, the magnetoeletric coefficients obtained through the measurement of single crystal magnetization [8] also showed a factor two in the magnitude of the asymmetry, after magnetoeletric switching from one state to the other, as illustrated in figure 1. Although the asymmetry in the magneto-electric susceptibility does not survive application of sufficiently high external fields, this is still evident as a metastable state or intermediate state for single crystal Cr_2O_3 without any adlayers. In light of the measurements reported here, this asymmetry in the switching field and/or in the magnitude of the exchange bias one domain state over the other may now safely be assumed to have a significant contribution from the surface magnetization once the boundary polarization is considered [1–3]. The possible existence of intermediate states occurring upon domain reversal must be considered. Interface dipole effects should be evaluated against the possibility of some frustration in the domain reversal in the region of an interface or surface. Finally, although they appear unlikely, different possible surface terminations cannot *a priori* be excluded.

Conclusion

This work shows that the placement of Cr_2O_3 single crystal in the single domain state, does not, *a priori*, lead to an identical boundary polarization for both domain states, if the equivalence of the two domains states is broken by an electrostatic interface dipole, i.e. contact with a conducting layer. This may be the origin of the variations in the magnitude of exchange bias, under some conditions, for the two different domains states.

Acknowledgements

This project was supported by the Semiconductor Research Corporation through the Center for Nanoferroic Devices, an SRC-NRI Center under Task ID 2398.001, and by the NSF through Nebraska MRSEC DMR-0820521 and DMR 0747704. The SPLEEM experiments were performed at the National Center for Electron Microscopy, supported by the Office of Basic Energy Sciences of the US Department of Energy under contract no. DE-AC02-05CH11231.

References

[1] Andreev A F 1996 *JETP Lett.* **63** 758
[2] Belashchenko K D 2010 *Phys. Rev. Lett.* **105** 147204
[3] He X, Wang Y, Wu N, Caruso A N, Vescovo E, Belashchenko K D, Dowben P A and Binek C 2010 *Nature Mater.* **9** 579–85

[4] Wu N, He X, Wysocki A, Lanke U, Komesu T, Belashchenko K D, Binek C and Dowben P A 2011 *Phys. Rev. Lett.* **106** 087202
[5] Hochstrat A, Binek C, Chen X and Kleemann W 2004 *J. Magn. Magn. Mater.* **272-276** 325–6
[6] Echtenkamp W and Binek C 2013 *Phys. Rev. Lett.* **111** 187204
[7] He X 2012 *PhD Thesis* University of Nebraska-Lincoln
[8] Martin T J and Anderson J C 1966 *IEEE Trans. Magn.* **2** 446
[9] Sahashi M and Nozaki T 2014 private communication
[10] Iyama A and Kimura T 2013 *Phys. Rev.* B **87** 180408(R)
[11] Rougemaille N and Schmid A K 2010 *Eur. Phys. J. Appl. Phys.* **50** 20101
[12] de la Figuera J, Vergara L, N'Diaye A T, Quesada A and Schmid A K 2013 *Ultramicroscopy* **130** 77
[13] Chen X *et al* Ultrathin chromia films grown with preferential texture on metallic, semimetallic and insulating substrates *Mater. Chem. Phys.* submitted
[14] Huggins C P and Nix R M 2005 *Surf. Sci.* **594** 163–73
[15] Sokolov A *et al* 2002 *Europhys. Lett.* **58** 448–54
[16] Cheng R, Komesu T, Jeong H-K, Yuan L, Liou S-H, Doudin B, Dowben P A and Losovyj Y B 2002 *Phys. Lett.* A **302** 211–6
[17] Bikondoa O, Moritz W, Torrelles X, Kim H J, Thornton G and Lindsay R 2010 *Phys. Rev.* B **81** 205439
[18] Wysocki A L, Shi S and Belashchenko K D 2012 *Phys. Rev.* B **86** 165443
[19] Wang X G and Smith J R 2013 *Phys. Rev.* B **68** 201402
[20] Gloege T, Meyerheim H L, Moritz W and Wolf D 1999 *Surf. Sci.* **441** L917–23
[21] Lübbe M and Moritz W 2009 *J. Phys.: Condens. Matter.* **21** 134010
[22] Tsymbal E and Kohlstedt H 2006 *Science* **313** 181
[23] Kim D J, Lu H, Ryu S, Bark C-W, Eom C-B, Tsymbal E Y and Gruverman A 2012 *Nano Lett.* **12** 5697–702
[24] Gruverman A *et al* 2009 *Nano Lett.* **9** 3539–43